1st Reading

International Journal of Modern Physics B
Vol. 29, No. 0 (2015) 1550186 (23 pages)
© World Scientific Publishing Company
DOI: 10.1142/S0217979215501866

World Scientific
www.worldscientific.com

Investigation of dielectric behavior of water and thermally aged of XLPE/$BaTiO_3$ composites in the low-frequency range

Lakhdar Madani*, Saad Belkhiat, Amine Berrag and Saad Nemdili

Laboratoire Dosage Analyse Caracterisation Haute Résolution,
Ferhat Abbas University Setif-1, Algeria
**madani_lakhdar10@yahoo.fr*

Received 30 November 2014
Revised 16 July 2015
Accepted 24 July 2015
Published DD MM 2015

Cross-Linked Polyethylene (XLPE) is widely used as insulation in electrical engineering, especially as cable insulation sheaths. In order to improve the dielectric properties susceptible to be modified under the effects of thermal aging and water in an absorption environment, polymers are mixed with ceramics. In this paper, the influence of barium titanate ($BaTiO_3$), on the dielectric properties of XLPE has been studied. Dielectric parameters have been measured using an impedance analyzer RLC (WAYNE KERR 6420 type). Fourier transform infrared (FTIR) spectroscopy, scanning electron microscopy and X-ray diffraction were used as characterization techniques. The study has been carried out on two samples of XLPE. A pure sample of each were studied as a unloaded samples to be compared with samples of 5%wt, 10%wt, 15%wt and 20%wt. $BaTiO_3$ loaded XLPE. Afterwards, the composites were subject to humidity and to thermal aging. The incorporation of $BaTiO_3$ 1°C does not modify the crystallinity and morphology of the XLPE and 2°C reduces the space charges therefore the dielectric losses. $tg\delta$, ε_r and loss index are measured. Frequency response analysis has been followed in the frequency range (20–300 Hz). Experimental results show well that $BaTiO_3$ as nano-filler improves the dielectric properties of XLPE but in excessive content can drive to the cracking and therefore to absorption of water.

Keywords: XLPE; composite; $BaTiO_3$ doped XLPE; thermal aging; micro-structural analysis.

PACS numbers: Author to provide

1. Introduction

Due to its excellent dielectric strength, low dielectric permittivity, low loss factor and thermomechanical behavior, cross-linked polyethylene (XLPE) has been used,

*Corresponding author.

for several decades, as an electrical insulating material in distribution; (especially underground), and transmission cables. XLPE has a high breakdown voltage but space charge formation in PE is an inherent characteristic. Under normal operating voltage stress, a series of partial pre-breakdown channels emanates from a region of exiting defect sites, in the form of gas cavities or conducting inclusions or intrusions in the insulation structure.[1] The space charge is an important factor in the degradation of polyethylene. Its accumulation in the defect sites can distort the electric field distribution in the polymer insulation matrix and results in reducing electrical strength such as carried out by Gonzalez-Benito *et al.*[2] Reduction of accumulated space charges and modification of their, its distribution is beneficial for the reliability of polymeric insulated high voltage device.[3] This challenge has led to the development of polymer composite systems. Composites potentially combine the processability and breakdown field strength of the polymer with the high dielectric constant of ceramic fillers.[4–6] The filler contributes to increase the effective dielectric constant of the composite system while not extensively compromising the high inherent breakdown strength of polymers.[7] Organic polymers have relatively low dielectric constant, usually within the range of 2–10.[8] To increase the dielectric constant, International standard norm recommends fillers with a permittivity that is higher than 14 such as barium titanate ($BaTiO_3$) or TiO_2. However, these fillers exhibit low electrical breakdown strength, consequently low breakdown voltage.[9] It is therefore expected that the breakdown voltage of the composite will be lower than that one of pure polymer.[7] Polymer matrix composites must be so prepared looking for synergy between the advantages of the polymers and the special characteristics of the fillers leading to unique properties. Lomax *et al.*[10] explain electrical properties improvement of $BaTiO_3$ composite based poly(etherimide) (PEI). $BaTiO_3$ ($\varepsilon_r = 3300$) nano-particles incorporation into PEI ($\varepsilon_r = 3.17$), results to obtaining a composite having a ε_r (between 3 and 10) versus volume fraction $BaTiO_3$. The permittivity value of the composite was in the range of that one required for the organic polymer.[8] The results were explained using the following equation:

$$\frac{\varepsilon_1 - \varepsilon_c}{\varepsilon_1 - \varepsilon_b}\left(\frac{\varepsilon_b}{\varepsilon_c}\frac{1}{\mu}\right) = 1 - P_{\mathrm{Par}}\,, \tag{1}$$

where ε_b, ε_1 and ε_c represent the relative permittivity's of PEI, $BaTiO_3$ nano-particles, and the nano-composite, respectively, while P_{par} is the volume fraction of the particles and μ is a parameter that depends on subtleties of the microstructure such as particle clustering and surface roughness. It was shown that due to the high ratio (1040) of the relative permittivity of $BaTiO_3$ to that of the PEI, the results were only weakly sensitive to $BaTiO_3$ relative permittivity at the volume fractions used. Otherwise, the dielectric constant of particles (ε_1) is size dependent and has an influence on the particle polarization in the composite through its effect on the local electric field Eq. (3). The mixture model given in Ref. 11 expressed ε_c as follows:

$$\log \varepsilon_c = P_{\mathrm{par}} \log \varepsilon_1 + P_{\mathrm{pol}} \log \varepsilon_b\,. \tag{2}$$

On the other hand, the mean electric field, E_{par}, acting on particles in a composite is given by Eq. (3),

$$E_{\text{par}} = \frac{3\varepsilon_b}{2\varepsilon_b + \varepsilon_1 + P_{\text{par}}(\varepsilon_b - \varepsilon_1)} E_{\text{app}}\,, \tag{3}$$

where E_{app} is the electric field, applied on the composite and P_{pol} is the volume fraction of the polymer. Looking to Eq. (2), mathematically ε_1 (of particle) has a low influence on the dielectric constant of a composite (ε_c) whereas P_{par} generally is lower in comparison with P_{pol}. Finally Eqs. (1) and (2) show well that ε_1 has little influence on ε_c. Nevertheless, ε_1 rises with increasing particle size but E_{par} rises with decreasing particle size.[11] However, the dielectric breakdown depends on the cumulative probability Eq. (4) of failure for a given dielectric strength E^2 such as:

$$P(E) = 1 - \exp\left[-\left(\frac{E}{E_0}\right)^{\alpha w}\right].$$

E_0 is the characteristic field with a 63.2% probability of failure. The exponent, α_w is related to the distribution of the defects present in the dielectric. The higher is this value, the narrower is the distribution. Decreased dielectric strength is commonly attributed (by literature) to matrix electric field intensification. So that, it is necessary to take into account that one of the main prerequisites to achieve the best performance of these composites is to ensure uniform dispersion of the particles within the polymer matrix, while the formation of aggregates, small voids, pores or even agglomerates of particles may lead to nondesired properties. Microscopic variations of permittivity may lead to local increase of electrical field in small volumes that might create partial discharges. These probable defects can be a favorable medium for space charge and for water absorption for the used composites in a humid medium. Under certain condition, if water diffuses, composite insulating cable or insulators can fail in service. The presence of water can cause brittle fracture and change significantly the electrical properties of the composite.[12] However, with respect to aging and degradation during service, thermo-oxidation and water treeing often originate the premature electrical breakdown of XLPE as electrical insulating material.[1,13,14] Estimation of the degree of aging is at present the most important task of diagnostic methods of polymer composites. Thermal aging and humidity cause an irreversible chemical and morphological change that may strongly reduce the properties of XLPE, and produce a limit to the service life of the power cable. Clearly, the effects of temperature must be determined in this area. Few studies on the doped XLPE have been found in the literature. Thermal aging of pure XLPE has been studied by Eddy *et al.*[15] They found that the material oxidation was characterized by a significant increase in the molecular mobility of the amorphous region. The increase in molecular mobility indicates that XLPE undergoes chain scission during thermal oxidation. Recently composite materials based on HDPE filled with $BaTiO_3$ particles, very appealing in the manufacture of electric and electronic systems such as insulators for cables, have been analyzed using SEM,

Fourier transform infrarer (FTIR) and stress–strain tests as a function of $BaTiO_3$ contents.[2] The decrease in resistivity and breakdown voltage have been attributed to increasing of $BaTiO_3$ amount. The breakdown mechanism was explained by the higher interaction between filler particles which leads to higher dipole moment in specific areas of the dielectric, where the electrical field is amplified. In the case of $BaTiO_3$ fiber/ PDMS composite and GPL/PDMS composite[7] the breakdown mechanism was explained by the stress concentration at the interfaces between the filler and the polymer matrix. When the high dielectric constant or high conductivity filler is added into the polymer, the electrical field in the polymer around the filler is much larger than that in the bulk. The most stressed part should be close to the edge of fillers and the local stress should increase with filler aspect ratio. Breakdown voltage is more likely to be initiated at these highly stressed regions than in the bulk polymer.

$BaTiO_3$ as a filler is insoluble in the water, and no changes were observed in morphology and composition of $BaTiO_3$ powders exposed to water[16]; whereas $BaTiO_3$ can be hydrothermally synthesized by conversion of TiO_2 in $BaTiO_3$.[17,18] Electrical strength, resistance to partial discharges and appearance of conducting path due to partial discharges, dielectric loss factor, resistivity or permittivity are the electrical properties which may be changed by filler addition. Small particles (nano-filler) of $BaTiO_3$ are used so that they contribute to reduced space charges, and so consequently field distortions. At the same time by filling them up, the filler reduces, inter-granular voids and pores expected during manufacturing process; thus reducing water absorption.[19]

Though, few of works have been carried out in low frequency concerning $BaTiO_3$ loaded XLPE composite, many studies have been carried out on the dielectric properties of the polyvinyl chloride (PVC).[15,20–22] Used in the electronic device, it has been studied in the ultra-low frequency range. Focusing mainly on relaxation phenomenon, matrix–ceramic $BaTiO_3$ composites have been examined by means of Broadband dielectric spectroscopy in $10^{-1} - 10^7$ Hz frequency range and over 30–160°C temperature range.[20] It was found that the activation energies were correlated to the changes of $BaTiO_3$ concentration in the composite. The relaxation features were typically studied in high frequency, as opposed to the few in low frequency. Dielectric relaxation has been extensively analyzed and has been reviewed in a number of articles.[23–25] As well, dielectric relaxation, linked to space charges, is very well studied in the literature.[18,26,27]

In this paper, $BaTiO_3$ composite based XLPE has been studied. $BaTiO_3$ nanoparticle (5%wt, 10%wt, 15%wt and 20%wt) were used in order to reduce the cumulative probability of failure and to ameliorate electric field distribution. Frequency response analysis and dielectric properties were performed. ε_r, $tg\delta$ and loss index were measured and compared with that one of pure XLPE. Noting that dielectric constant is defined as $\varepsilon_r = C/C_v$ where C is the capacity of material under test and C_v is the capacity of air. Under an alternate electric field, the dielectric constant of material can be expressed by a complex permittivity such $\varepsilon = \varepsilon'(\omega) - j\varepsilon''(\omega)$.

Table 1. Content of XPLE/$BaTiO_3$ composite in weight percent.

Samples	1	2	3	4	5
Polymer (XLPE) [.wt%]	100%	95%	90%	85%	80%
$BaTiO_3$ [.wt%]	0%	5%	10%	15%	20%
$BaTiO_3$ [volume fraction]	0%	0.8%	1.72%	2.7%	3.79%

The dielectric loss tangent is defined as $tg\delta = \varepsilon''/\varepsilon'$ and the dielectric loss index as $\varepsilon'' = \varepsilon' tg\delta$.

We showed that $BaTiO_3$ as nano-filler improved the dielectric properties of XLPE but in at higher content, it can lead to cracking of the composite and therefore to absorption of water.

2. Experimental Section

The composition of the studied samples is given in Table 1. The basic element was the XLPE (4201 Union Carbide (USA) type), mixed with an antioxidant assuring the thermal stability and with dicumyl peroxide cross as linking agent.

Two types of samples (unloaded XLPE and $BaTiO_3$ loaded XLPE) were elaborated in conformity with International Standard Norm.[4] $BaTiO_3$ grains size was of order 70 nm. It is obtained from ALFA AESAR. The formulation has been mixed in a two-roll mixer during 20 min at a temperature of 120°C. After that the vulcanization of the mixture was conducted under a heating press at a pressure of 120 kg/cm^2.

The sample was prepared as sheets of predetermined thickness. The sheet is then cut into square of 10 cm $\times$ 10 cm and 0.4 mm as thickness. Some composite samples were aged at 100°C during 200 h. Other samples were immersed in water for 72 h and thereafter they were dried in free air at room temperature in order to study the influence of water on the dielectric properties of the composite. FTIR spectroscopy (JASCO FT/IR4200 type), scanning electron microscopy (SEM, JEOL JSM model 7001F) and X-ray diffraction (BRUKER ADVANCE X-RAY SOLUTIONS) were used to characterize the structure of the elaborated composite. FTIR is a device of JASCO FT/IR4200 type working in the frequency range 600 cm^{-1} to 4000 cm^{-1} and with 0.5 cm^{-1} as maximum resolution. The dielectric response of the samples was measured on an impedance analyzer RLC (WAYNE KERR 6420 type) working in the range frequency up to 10 MHz. The samples are then inserted between two plane electrodes made of copper. The capacitor representing the sample is afterwards submitted to an alternating electric field of 1 V/m. $tg\delta$, ε_r and loss index have been measured. The measurement error was $\pm 0.05\%$.

3. Experimental Results

Among many hypotheses about the mechanism of the water influence on the lifetime of cable, it can be outlined that the water penetrates into cable insulation from

the outside and condenses at defects such as voids or impurities.[28] As the XLPE composite is also used in the network insulator, the samples were rather aged during hours under the effects of temperature and water absorption. The polymer insulation around those defects will be thus mechanically stressed by the pressure of water, or as the effect of Maxwell's stress which forms micro-cracks leading to local defects in the cable insulation or the insulator surface. The time dependent aging under different temperature and water effects was studied and the results are given in the next sections.

3.1. *$BaTiO_3$ effect On humidified XLPE*

The content of the absorbed water in the samples (typical size 0.4 g) has been measured by an analytical balance (KERN-ABT 120-4M, precision $+/-2.10^{-4}$ g). The measurement results are given in Fig. 1. Though $BaTiO_3$ is profoundly insoluble in water, water does adsorb onto its surface. It is anticipated that much of the surface water is removed during rolling at 120°C, some may remain. This may contribute to the modest increase in water as a function of $BaTiO_3$ content.[16,29] There is less of water absorption into the composite. Water absorption tends rather towards a slight average increasing as a function of $BaTiO_3$ content. The measurements oscillation as seen in the curve (Fig. 1) can be attributed to the formation of aggregates or small voids or pores or even agglomerates of particles which may lead to water absorption such as carried out in Refs. 1, 12 and 19. However, the result will be developed in the following sections as that one relative to SEM characterization. It is expected that more filler content greater more the cells between the grains of polymer matrix are reduced. Maximum of water absorption was measured into the

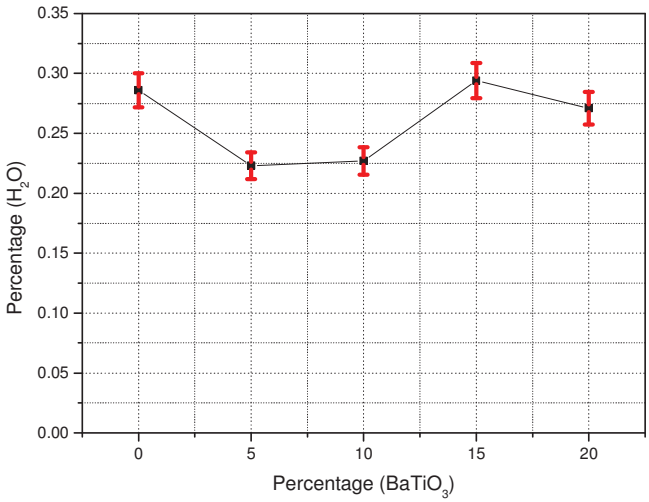

Fig. 1. %wt of water absorption measured on samples of $BaTiO_3$ loaded XLPE.

sample number four (15%wt $BaTiO_3$). The study was focused (point of view structure characterization) especially on the four first samples whereas the percentage of humidity of the sample number five was smaller than that of the sample number four.

3.2. *$BaTiO_3$ effect on permittivity*

As seen in Fig. 2, the permittivity is similar but increases between samples with 0%, 5% and 10% with marked increases in 15% and again 20% $BaTiO_3$. All samples maximize ε_r at 50 Hz (4.4–6.5) and reduce to values of 2.27–4.5 at 300 Hz as a function of $BaTiO_3$ content. ε_r increases when the additive content increases. This is in agreement with literature.[2,5,9,30] A first minimum was obtained at the frequency 35 Hz. After that ε_r increases quickly to reach a maximum value (between 4.4 and 6.5) at 50 Hz. Afterwards, ε_r decreases to stabilize between 2.27 and 4.5 into the range [100–300 Hz]. The ceramics such as $BaTiO_3$ are known for their high permittivity. This is clearly seen in Fig. 2 showing that the permittivity of $BaTiO_3$ loaded XLPE increases comparatively with unloaded sample [Fig. 2(a)] even for the samples subject to humidity [Fig. 2(c)] and for the samples subject to thermal aging [Fig. 2(b)]. $BaTiO_3$ contributes to the ε_c enhancement. Aging the sample at 100°C during 200 h seems to have little effect on the permittivity of the composite whereas the results are closer to that one obtained before thermal aging. The results are similar to that one carried out in Ref. 30. Thermal aging of the unloaded sample has been characterized by 13% as reduction of ε_r [see Fig. 2(b)]. ε_r decreases of about an average of 12% for the sample number two. However, a reduction of 9% and 6% were obtained for the samples number three and four, whereas ε_r was reduced on the order of 3% for the sample five in comparison with the results obtained with the same samples [Fig. 2(a)] before thermal aging, see Table 1. The results are reverse to that expected whereas the permittivity would increase after aging. Thermal effect rather seems to reduce the defects due to elaboration process of the composite and therefore reduces the conductivity of the composite.

However, an increase of about 18% of ε_r is observed when the samples two, three and four are subjected to water, ε_r increases of 13% for the samples number five [Fig. 2(c)] in comparison with the results obtained with the same samples before thermal aging [Fig. 2(a)]. However, ε_r of unloaded sample was 22% greater under water effect, comparatively with the same sample before water absorption. Also, the dielectric constant was so higher in the unloaded sample than that loaded whereas $BaTiO_3$ particles (few soluble in water) were incorporated into the defect sites, as small voids or pores of XLPE. Incorporation of $BaTiO_3$ reduces the voids or pores in the composites, therefore reduces water absorption and increases ε_r whereas water is also a strongly polar medium having higher ε_r which the value is closer to 80 at ambient temperature. The voids or pores as defects in the composite can be also filled of water in addition of $BaTiO_3$ enhancing, thus the composite permittivity.

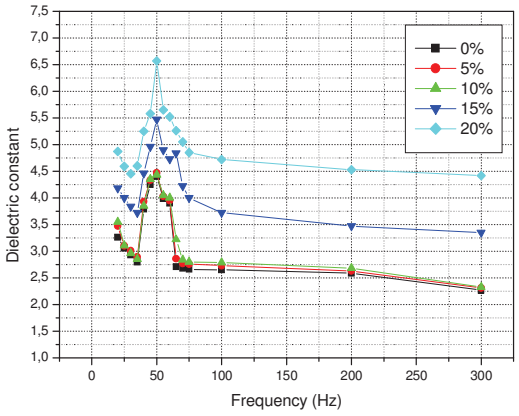

(a)

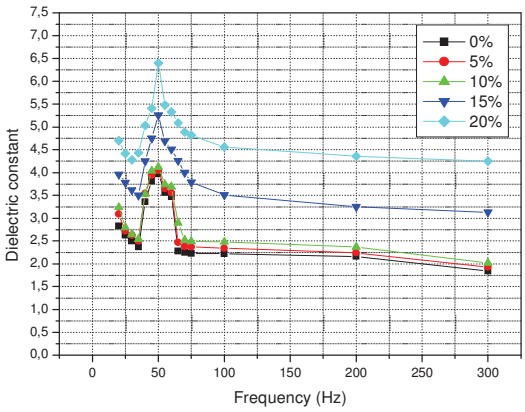

(b)

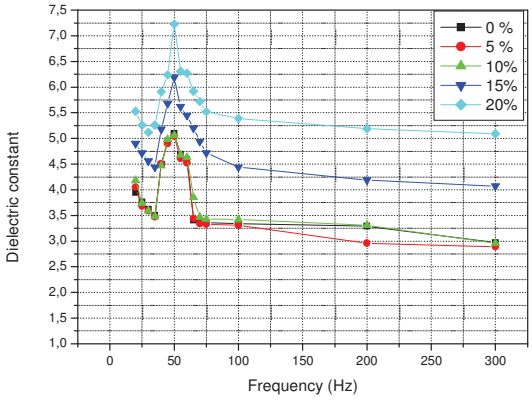

(c)

Fig. 2. (a) ε_r of unloaded and $BaTiO_3$ loaded XLPE, (b) ε_r after thermal aging and (c) ε_r of $BaTiO_3$ loaded XLPE after water absorption.

3.3. *BaTiO$_3$ effect on loss factor*

The lower value of $tg\delta$ was obtained for the loading contents of $BaTiO_3$, see Table 1. We can well see that $tg\delta$ decreases when $BaTiO_3$ content increases. The decrease of $tg\delta$ is more remarked in the samples containing 15% and 20% of $BaTiO_3$.

Loss factor $tg\delta$ as a function of the frequency for the unloaded and $BaTiO_3$ loaded XLPE sample is shown in Fig. 3(a). In first, the loss factor increases rapidly and a first maximum occurs at the frequency 30 Hz. After that it decreases at 35 Hz. A rapid increasing again of $tg\delta$ to a maximum located at 50 Hz. It is so seen that the relaxation phenomenon is characterized by two peaks located surroundings 30 Hz and 50 Hz, respectively. This latter value depends on the $BaTiO_3$ content in the sample.

Furthermore, and from 50 Hz, $tg\delta$ decreases rapidly until the frequency 75 Hz. After this latter value, $tg\delta$ decreases slightly and tends respectively (for the different contents of $BaTiO_3$) towards lower values at 300 Hz (see Table 2). Dielectric losses are due essentially to space charge because of interfacial polarization originate of defects such as voids and pores expected during composites elaboration. The results show, so that more nano-filler content ($BaTiO_3$) is greater, more dielectric losses is smaller. $BaTiO_3$ contributes so for reduction of accumulated space charge and for modification of its distribution density.

The obtained curves, concerning the samples having been aged under temperature and humidity effects, were similar to that of the unloaded sample of point view form [Figs. 3(b) and 3(c)]. $tg\delta$ decrease in the same way than that one of composites before aging and before humidity effect. Only $tg\delta$ increases in comparison with the results of the same samples before aging (see Table 2).

Under thermal aging $tg\delta$ decreases from 0.44 to 0.172 at 50 Hz and from 0.23 to 0.09 at 300 kHz when $BaTiO_3$ content increases from 0 to 20%wt (see Fig. 3(b) and Table 2). Referring to literature, space charge decreases at high temperature. One expected so that the losses could have been lower than that found; but as the loading is of ferroelectric type, thermal polarization can be induced under the

Table 2. $tg\delta$ as a function $BaTiO_3$ content.

Sample	0%wt $BaTiO_3$	5%wt $BaTiO_3$	10%wt $BaTiO_3$	15%wt $BaTiO_3$	20%wt $BaTiO_3$
			Unloand $BaTiO_3$ loaded XLPE		
$tg\delta$ (50 Hz)	0.273	0.244	0.233	0.126	0.085
$tg\delta$ (300 Hz)	0.045	0.03	0.028	0.013	0.01
			After thermal aging		
$tg\delta$ (50 Hz)	0.44	0.37	0.36	0.25	0.172
$tg\delta$ (300 Hz)	0.23	0.20	0.18	0.12	0.09
			After water absorption		
$tg\delta$ (50 Hz)	0.49	0.42	0.41	035	0.3
$tg\delta$ (300 Hz)	0.28	0.20	0.22	0.26	0.225

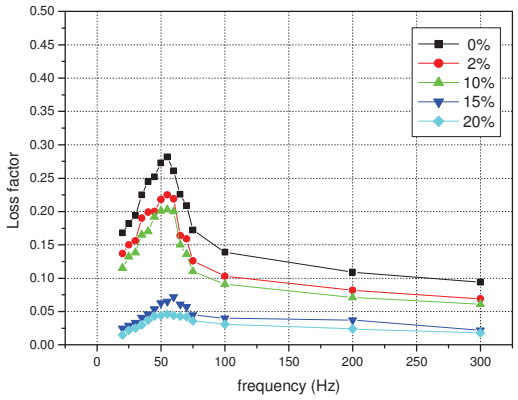

(a)

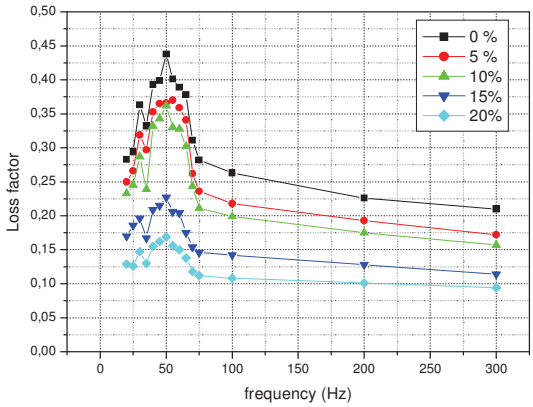

(b)

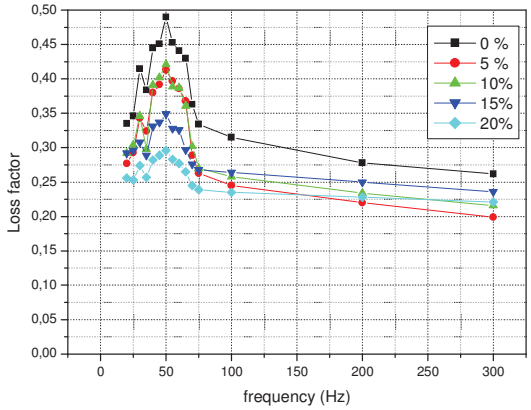

(c)

Fig. 3. (a) Loss factor of unloaded and $BaTiO_3$ loaded XLPE, (b) Loss factor after thermal aging and (c) Loss factor after water absorption.

temperature effect in the grains interface in addition of the space charge due to interfacial polarization originate of defects and therefore increases $tg\delta$.

However, under humidity effect $tg\delta$ decreases from 0.49 to 0.3 at 50 Hz and from 0.28 to 0.2 at 300 Hz (see Fig. 3(c) and Table 2). It is greater, as seen in Table 2, in the case of water absorption. Water presence leads to more space charge, while it is a polar liquid which can locate in defect sits and even in interface matrix/loading grains.

In the two cases, under temperature and humidity effects, $tg\delta$ increases almost two times in comparison with the obtained results before aging. We can see that even after aging the losses remain acceptable and closer than the one other. Small particles of the nano-filler lead so to larger relative contact areas with matrix material and are so responsible for the improvements observed in the dielectric properties of the composites..[19] The obtained results were in agreement with literature.[5,9,30]

3.4. *$BaTiO_3$ effect on loss index*

Figure 4 represents the evolution of loss index as a function of the frequency. We can see in Fig. 4(a) the obtained results on the unloaded samples before and after doping. The higher loss index has been measured in the pure sample (0% $BaTiO_3$). It decreases, when $BaTiO_3$ content increases. Afterwards dielectric loss increases with frequency in the range (20–300 Hz). The relaxation phenomenon is characterized by two peaks located surroundings 30 and 50 Hz respectively. The results show, so that the addition of $BaTiO_3$ significantly reduces the loss index in the samples strongly filled (15%wt $BaTiO_3$ and 20%wt $BaTiO_3$). It was 1/3 the value in the 20% by mass than the unloaded sample. Furthermore, the thermal aging [Fig. 4(b)] affects most of the loss index. The maximum losses at 300 Hz change from $13.2.10^{-10}$ W/cm^3 to $16.6.10^{-10}$ W/cm^3 as a function of the $BaTiO_3$ content.

The greater value of the dielectric loss corresponds to the unloaded sample, before and after thermal aging [Figs. 4(a) and 4(b)]. The lower value has been obtained on the sample number five whereas the value was $\sim$3 times greater [Fig. 4(b)] than in the case of the unloaded sample [Fig. 4(a)]. Concerning, the humidity effect, the measurement results are represented in the Fig. 4(c). Dielectric loss measured on the sample five was equal to $46.8.10^{-10}$ W/cm^3 at 300 Hz. This value was $\sim$7 times greater than that one in the case of the unloaded sample. However, $23.9.10^{-10}$ W/cm^3 as lower value of losses at 300 Hz has been obtained for the sample number two. Thus, the strongly doped samples were more affected by the water absorption.

3.5. *Micro-structural analysis of samples*

3.5.1. *Fourier transform infrared spectroscopy*

Figure 5 shows FTIR spectra of pure XLPE and XLPE/$BaTiO_3$ composite. The absorption spectra [Fig. 5(a)] exhibits different absorptions, located at 2920 and

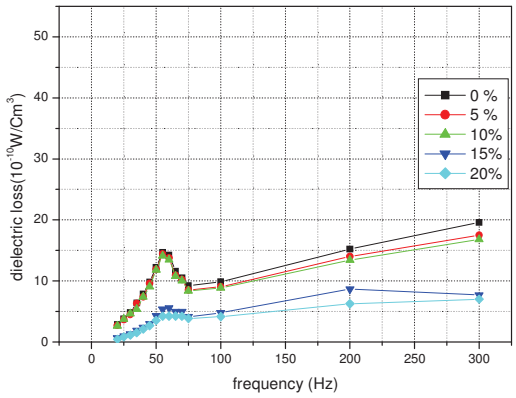

(a)

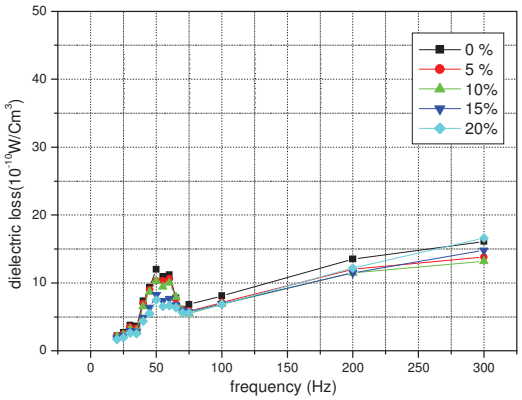

(b)

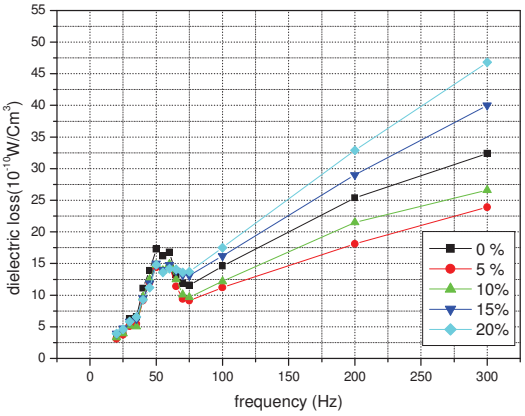

(c)

Fig. 4. (a) Loss index of unloaded and $BaTiO_3$ loaded XLPE, (b) loss index after thermal aging and (c) loss index after water absorption.

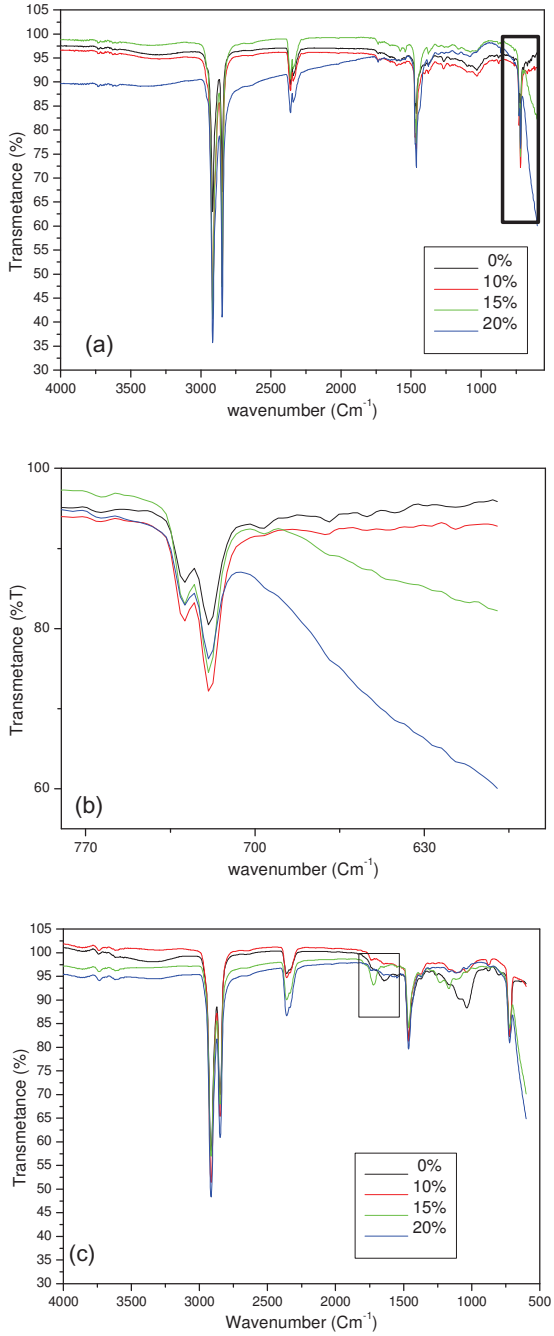

(c)

Fig. 5. FTIR spectra of pure XLPE and XLPE/ $BaTiO_3$ composite (a) before thermal aging, (b) zoom of the part in the rectangle spectra Fig. 5(a) and (c) after thermal aging.

2850 cm^{-1}. They are respectively the characteristics of asymmetrical and symmetrical stretching of methylene groups. Other peaks were located at 2300 and 2400 cm^{-1}. These latter were observed in all samples, before and after loading and aging. They come probably from CO_2. They are more resolved than that one carried out in the Ref. 1. Otherwise, the absorption band located at 1460 and 720 to 730 cm^{-1} is due to C–H bending. We can well see the zoom of the part surrounded by a rectangle [Fig. 5(b)] where the peaks located at 720 and 730 cm^{-1} are well resolved. These results are in agreement with literature.[1] Similar absorption bands are also observed for $BaTiO_3$ loaded XLPE. There is no absorption band recorded in the range 700 to 400 cm^{-1}. The composites spectra particularly that one characteristic of the samples number four (15%wt $BaTiO_3$) and number five (20%wt $BaTiO_3$) tend to decrease in amplitude for probably possible apparition of absorption peaks expected towards 570 cm^{-1}. Two broad absorption peaks characteristics respectively of Ti–O vibrational mode and $BaTiO_3$ such as carried out in the literature[30,31] were so expected at 570 and 440 cm^{-1}. These ones cannot record with the used IR spectrometer whereas 610 cm^{-1} [see Fig. 5(b)] is its short wave number limit. The other absorption peak located at 1474 cm^{-1} corresponds to CH_2 bending mode. It is due to the crystalline phase such as found in the literature.[2,32] A small absorption peak [Fig.5(a)] was also appeared between 1250 and 1000 cm^{-1} for both before and after doping. The same absorption band has been found in Chonung *et al.*'s work.[1] Otherwise, the peaks characterizing the composites are located in the same wave number than that one of pure XLPE. No chemical alteration induced by $BaTiO_3$ has effect on XLPE.

A new small absorption peak located at 1720 cm^{-1} is more visible for the sample number four (15%wt $BaTiO_3$). This one is surrounded by a square in the spectra. It is due to the carbonyl group formation, similar to that found in Ref. 14. It is the characteristic of detecting oxidation in XLPE. Otherwise, the absorption band observed between 1250 cm^{-1} and 1000 cm^{-1} is more resolved particularly for the sample one. This latter has been attributed to the duration of aging. For the sample four(15%wt $BaTiO_3$) we can see that is a few less resolved and which shift towards 1464 and 1474 cm^{-1} that the Refs. 2 and 32 attributes to CH_2 bending mode due respectively to the amorphous phase and the crystalline phase. If we refer to the Ref. 2 and to Fig. 5(a). $BaTiO_3$ content does not originate from this peak (1464–1474 cm^{-1}) whereas the calculations made by Gonzalez-Benito *et al.*[2] have shown that the amorphous content remains almost stable (0.50%) for various $BaTiO_3$ content incorporated in HDPE. The shifting of the absorption band towards high wave number is so rather attributed to increasing crystalline phase under temperature effect. This result explains so $tg\delta$ decreasing under thermal aging.

3.5.2. *Scanning electron microscopy characterization*

The surface morphology of pure XLPE as well as $BaTiO_3$ loaded XLPE composite has been studied using SEM. The surface morphology observed by SEM is shown in

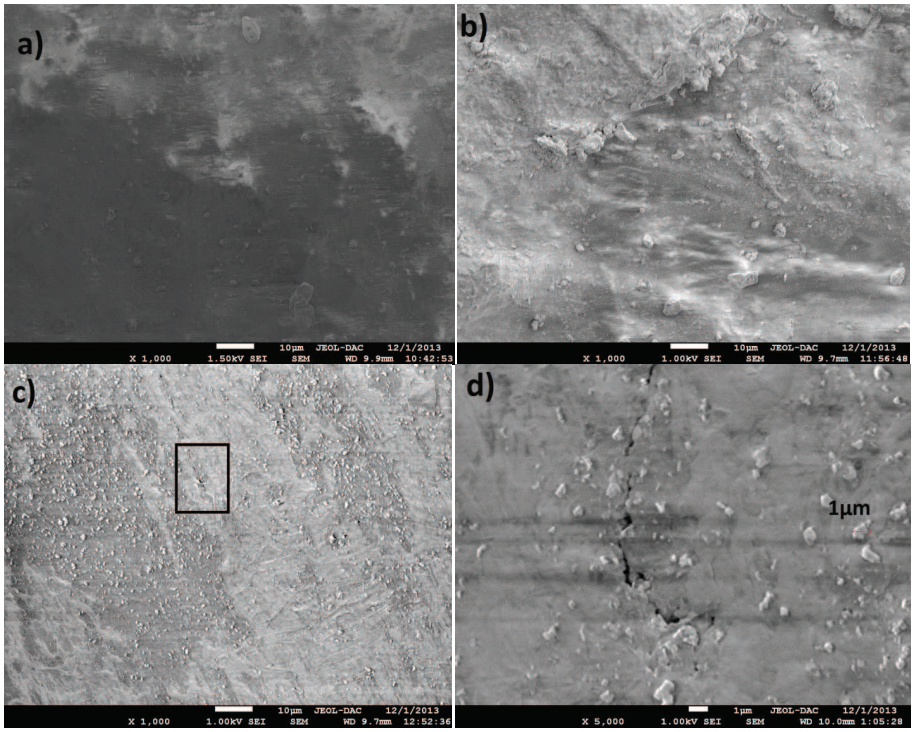

Fig. 6. SEM micrograph of (a) pure XLPE, (b) 10%wt $BaTiO_3$ loaded XLPE, (c) 15%wt $BaTiO_3$ loaded XLPE and (d) zoom of zone picked by square SEM image Fig. 6(c).

Fig. 6. We can see the SEM image of pure XLPE [Fig. 6(a)] which is characterized by a dark matrix where small bright domains are uniformly dispersed. However, the SEM image of the sample three (10%wt $BaTiO_3$) [Fig. 6(b)] as we see, is brighter and the grains dispersion of $BaTiO_3$ was also uniform. Otherwise, we observe a greater brightness and uniform distribution of $BaTiO_3$ grains in the SEM image of the sample number four (15%wt $BaTiO_3$) [Fig. 6(c)]. SEM image [Fig. 6(d)] shows the zoom of the zone picked out by a square [Fig. 6(c)]. The SEM image [Fig. 6(d)] shows the occurrence of small voids or pores (fissure) in the sample four. On the contrary, in the samples two (5%wt $BaTiO_3$) and three (10%wt $BaTiO_3$), the particles of filler present relatively a good dispersion in the XPLE matrix. We can see few particles agglomeration; therefore few of porosity were observed. The incorporation more than 10%wt $BaTiO_3$ can drive so to fissure. The same result has been carried out in the Ref. 30. EDS of pure XPLE and 15%wt $BaTiO_3$ loaded XLPE are given in Fig. 7. The ratios of Ba and Ti in the composite were respectively (7.95%) and (8.66%). The SEM images show well there are fissures and pores in the samples. This effectively explains the water absorption and space charge accumulation in the defect sits and therefore one confirms the results obtained concerning ε_r, $tg\delta$ and loss index.

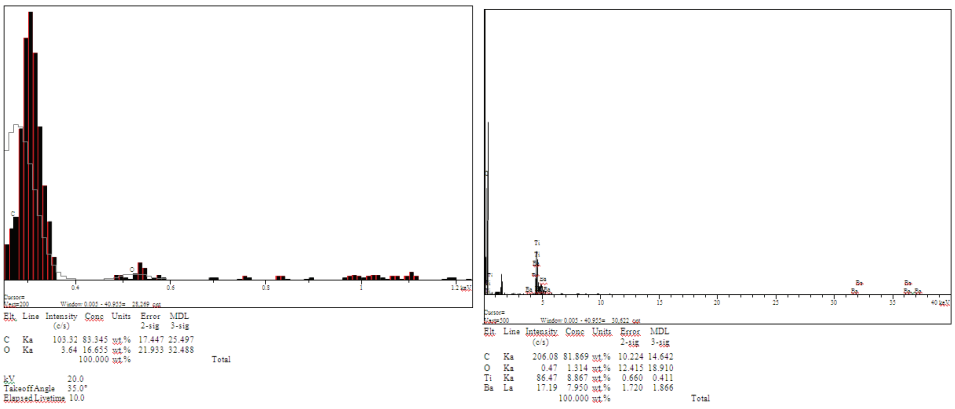

(a) (b)

Fig. 7. EDS of (a) pure XLPE and (b) 15%wt $BaTiO_3$ loaded XLPE.

The surface morphology of unloaded XLPE as well as $BaTiO_3$ loaded XLPE composite has been studied. In order to identify any variation in percentage crystallinity of the film samples or addition of new phases, X-ray diffraction analysis is presented in the next section.

3.5.3. *X-ray diffraction*

In order to investigate the stability of crystal structure of $BaTiO_3$ during the process of composite preparation, XRD measurements were carried out. Grains size of $BaTiO_3$ was evaluated to 70 nm. The XRD patterns of pure XLPE material and 10%wt/20%wt $BaTiO_3$ doped XLPE are shown in Fig. 8(a). The XRD spectrum characteristic of the XLPE specimen showed three peaks at 21.5°, 23.9° and at 36° which are characteristics of planes 110, 200 and 020 similar to the reference code (00-040-1995). For this X-ray diffraction pattern, the crystallinity was evaluated as 56 as that found in the literature.[33] Otherwise the crystallinity of 1%wt, 5%wt, 10%wt and 20%wt $BaTiO_3$ doped HDPE was evaluated to 50–53% in Ref. 2. Our results are so in agreement with literature.

Otherwise, the XRD spectrum of the composite is the characteristic of a cubic symmetry in which the parameter is equal to 3.9958 Å and the reflection peaks at 2θ (22.25°, 31.7°, 39°, 45.34°, 51.1°, 56.32° and 65.98°) correspond to (100), (110), (111), (200), (210), (211) and (320) diffraction planes, respectively and similar to reference code (01-075-2121). No change of the $BaTiO_3$ XRD pattern in the composite. This means that no change has occurred in the crystallinity of the material or no appearance of other new phase in the material. It can be deduced from these XRD patterns that there is no undesired interaction at the interface of $BaTiO_3$–XPLE upon dispersion. The same results have been carried out by other authors.[30,31] The XRD pattern of Fig. 8(b concerns the composites after thermal

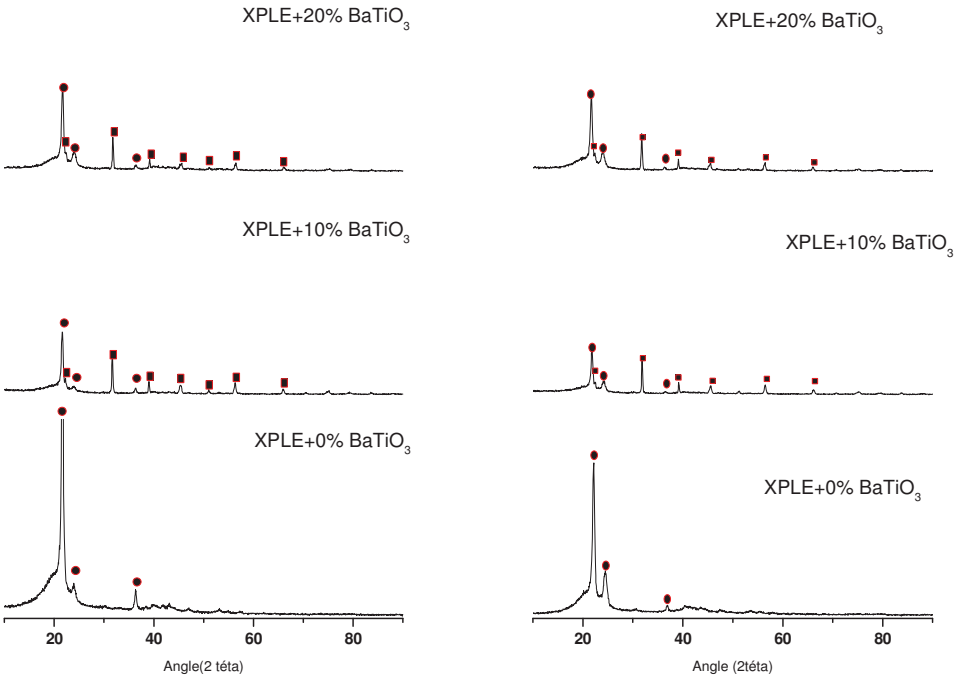

(a) (b)

Fig. 8. Angle X-ray diffraction pattern of pure and doped XLPE specimen (a) before aging and (b) after aging. (XPLE, $BaTiO_3$).

aging. No change in the spectrum as we can see. The composite crystallinity remains stable after being subjected to 100°C during 200 h.

4. Discussion

The influences of $BaTiO_3$ as nano-filler, of temperature and of water absorption on XLPE dielectric properties were analyzed. Generally, the literature agrees that ε_r and $tg\delta$ depends on the physical, chemical and structural changes of PE during service. In order to ameliorate PE performances novel polymeric composites containing ceramic powder have been developed.[6,35] In electrical engineering area, it is necessary to understand the dielectric behavior of the aged cables or insulator surface.[36–38] The temperature, therefore the ionic conduction mechanism of polymers was one of the most studied fields.[15,22] Electrical conductivity of polymer increases with increasing temperature.[15] Otherwise, in Ref. 22 the electric conductivity was found to be decreasing with increasing $BaTiO_3$ content. This one was explained as reducing of space charge (due to the capturing behavior of the ceramics) in the PVC matrix. The main current carriers were attributed to free ions from ingredients used in polymerization reaction of PVC, such as the stabilizer, as well as ingredients in the plastifier itself. In the case of our work, ε_r increases and $tg\delta$ decreases when the

nano-filler content increases (see Fig. 2). As the samples of this work were elaborated in the same conditions that one of the Ref. 22, one of plausible explanation for the increasing of ε_r with $BaTiO_3$ content [Fig. 2(a)] can be the conductivity of the $BaTiO_3$ nano-particles incorporated in the inter-granular interfaces of XLPE. However, after thermal aging [Fig. 2(b)] ε_r decreases very slightly (on the order of 3%) in comparison with the results obtained before thermal aging [Fig. 2(a)]. The similar result has been carried out in Lomax *et al.*'s works[10] whereas ε_r values were on the order of 5% higher than the values for the heat-treated PEI. The reason seems to be not obvious as it is said in the Ref. 10. However we attribute the values difference of ε_r (before and after thermal aging) to reducing impurities (such gas cavities or conducting inclusions) in XLPE under the temperature effect as also the possible reducing of the small pores and voids volume in addition of $BaTiO_3$. The result is in fact in correlation with that one found concerning the increasing of crystalline phase under temperature effect [see FTIR spectra Fig. 5(c)]. Otherwise, ε_r increases also slightly after water absorption [Fig. 2(c)] in comparison with the unloaded samples [Fig. 2(a)] while water is a polar medium. The increasing of ε_r is in agreement with results found in literature.[2,15,16,28,29] Equation (1) and the data of the Ref .10 can be used to calculate the permittivity (ε_c) of the composite whereas the composite is similar to that studied in this paper only PEI ($\varepsilon_b = 3.17$) was substituted by XLPE ($\varepsilon_b = 2.27$). ε_b equals to 2.27 was taken as average value measured in the range 75–300 Hz [see Fig. 2(a)]. The given value by XLPE cable manufacturer was 2.2 to 2.4. Our measured value was so in the required range. Table 3 gives the calculated value of ε_c using Eq. (1), for two frequencies, 50 and 300 Hz versus the weight fraction of $BaTiO_3$.

The ratio of the relative permittivity of the $BaTiO_3$ ($\varepsilon_1 = 3300$) to that for the XLPE, is large $R\varepsilon = 1320$. Effectively due to the high ratio Re of the relative permittivity, the result is weakly sensitive to $BaTiO_3$ relative permittivity such as predicted by Lomax *et al.*[10] For the three first samples respectively containing (0%wt $BaTiO_3$, 5%wt $BaTiO_3$ and 10%wt $BaTiO_3$ as loading), $\varepsilon_{c\,\mathrm{theo}}$ is closer to $\varepsilon_{c\,\mathrm{exp}}$ while these samples present no fissure and less aggregate than the samples four and five such that it has been characterized by SEM. The difference, as we can see between $\varepsilon_{c\,\mathrm{theo}}$ and $\varepsilon_{c\,\mathrm{exp}}$, is greater than that one of the first samples. The results can be confirmed using Eq. (2). ε_c value of the composite was located in the range required for organic polymers.[8]

Table 3. Composite permittivity (ε_c) measured and calculated.

Volume fraction	Weigh fraction	$\varepsilon_{r\,\mathrm{exp}}$ at 50 Hz	$\varepsilon_{r\,\mathrm{theo}}$ at 50 Hz (4.4)	$\varepsilon_{r\,\mathrm{exp}}$ at 300 Hz	$\varepsilon_{r\,\mathrm{theo}}$ at 300 Hz (2.27)
0	0%	4.4	4.43	2.27	2.32
0,008	5%	4.47	4.55	2.31	2.4
0,0172	10%	4.43	4.69	2.33	2.49
0,0270	15%	5.47	4.84	3.35	2.55
0,0379	20%	6.57	5.01	4.42	2.64

Otherwise, the electric field effect on the composite is expressed by Eq. (3). Mathematically, we can deduce that E_{par} acting on particles in composite will be smaller than the applied electric field E_{app}. E_{par} has been calculated in Ref. 11. The authors found that E_{par} increases when grain size decreases. The nano-filler using can increase so E_{par}, consequently we can approach the breakdown voltage of the composite to that one of XLPE (without or lower defects). However, the characteristic field E_0 [included in Eq. (4)] of composite is the electric field with 63.2% probability of failure. This one has been calculated in Ref. 10 for different volume fraction (or weight fraction) of $BaTiO_3$ in PEI. E_0 decreases as the nano-particles content increases. $BaTiO_3$ contributes so to increase the breakdown field. Nevertheless, E_0 depends especially on α_w values whereas higher this value, the narrow the distribution of the defects present in the dielectric, higher is E_0. On the other hand higher was weight fraction of $BaTiO_3$, lower was α_w and lower was E_0. Lower value of α_w signifies less of defects consequently less of space charge accumulation, and less of distorted electric field. Therefore, $BaTiO_3$ incorporation contributes to reduce P(E). We can conclude that in order to increase the breakdown field of the composite, it is necessary and indispensable in first to master elaboration process of the polymer or of the composite to reach the lower cumulative probability of failure P(E) Eq. (4) for a given electric field.

However, in this paper the samples were thermally aged at 100°C for 200 h (aging in the time as in Ref. 28 and 39 and immersed in water during 72 h. Afterwards the sample was dried in order to study the influence of water on the dielectric parameters all in remaining in the environmental conditions of insulating. The low absorption of water and its effect on the dielectric parameters modification are rather attributed to the elaboration defects such as shown in the Fig. 6. We can well see the fracture of the sample in Fig. 6(d). These ones contribute therefore to storage of water and to the interfacial polarization. However, the decreasing of the loss factor [Fig. 3) and loss index (Fig. 4) with $BaTiO_3$ content increasing is attributed to the space charge reducing in the bulk of the sample such as carried in the literature.[40] The molecular dipoles (may be) created by microscopic displacement of space charge were so lowered. The loss factor, is so reduced when $BaTiO_3$ particles (up 10%wt) are incorporated in XLPE. In the case of the samples three, four and five [Fig. 3(c)], in the range 100–300 Hz, the loss factor increases again. It is known that the dielectric loss depends on electronic, ionic, dipole-orientation and space charge polarizations especially in low frequency. As water is a polar medium, it contributes to space-charge polarization, therefore to enhance $tg\delta$.

Referring to the obtained results using various characterization techniques (IR spectroscopy, SEM and XRD) we deduce that the incorporation of $BaTiO_3$ does not modify the crystallinity and morphology of the XLPE. The XRD pattern of pure and loaded XLPE as well before than after aging is remained stable (without change) see Fig. 8. No chemical alterations are recorded in the composite. However, IR absorption spectra characterizing the samples before thermal aging also

remained stable [Fig. 5(a)] except for the short wave number (towards 610 cm^{-1}) where we observe the tendency to obtain peaks characteristic of $BaTiO_3$. The results are similar to that one found in the literature.[1,2,15,30,34,41] $BaTiO_3$ in the composites contributes so rather to reduce the defects and constitutes therefore a new phase located at the inter-granular interface of XLPE. Thus the system XLPE/$BaTiO_3$ leads to lower the mobility of the XLPE macromolecular segments as shown in Ref. 22.

However, small changes have been observed after thermal aging. The corresponding IR absorption spectra present new peaks located at 1720 cm^{-1} and surrounding 1250 cm^{-1} [Fig. 5(c)]. The absorption band recorded between 1250 and 1000 cm^{-1} was more resolved particularly for the sample one and less resolved for the sample four. This is shown that the temperature impact was greater on the unloaded sample than on the doped sample number four. The peak located at 1720 cm^{-1} characterizes the presence of the oxidative products (carbonyl group). It is the characteristic of XLPE oxidation. This was recorded only in the sample four while fissures have been observed by SEM [Fig. 6(c)]. The sample was more sensitive to temperature effect. However that one located around 1250 cm^{-1} characterizes the thermal aging effect such as carried out in Ref. 1. It was attributed to temperature and duration of aging. Finally, the results show well that the composite was less sensitive to thermal aging. Otherwise, spectra evolution is in correlation with the change of dielectric properties whereas loss index decreases [Fig. 4(b)] and $tg\delta$ increases [Fig. 3(b)] in comparison with the results before thermal aging [Figs. 4(a) and 3(a)], respectively. On the other hand the dielectric losses increase under humidity effect [Fig. 4(c)]. This is seen in the SEM image [Fig. 6(d)] that the fissure is one of defects originate water absorption. As water is a strongly polar medium, whereas $\varepsilon_{r\,\mathrm{water}}$ is, of the order of 80–83, the conductivity of the composite will be greater. The phenomena of space charge and the different polarization types (orientation and interfacial) related to the density of polymer-filler and water molecule will be greater whereas these polarizations induce most of losses and contribute to relaxation phenomena especially in low frequency.

The relaxation peaks often were studied in high frequency (some kHz to MHz), and few in low frequency.[1,42] Among, that one found in the literature[21] concerns $BaTiO_3$ loaded PVC. The study has been carried by Felix *et al.*[21] in the temperature range 27–68°C and the frequency scale 10^{-4}–10^{2} Hz. The relaxation peak has been obtained between 10^{-4} Hz and 1 Hz respectively at 27°C and at 68°C. The relaxation frequency shift towards higher frequencies with the increase of the temperature. This moving of relaxation peak as a function a temperature was indicated also in the work's[39]; only the shape and magnitude of the formed peaks remain more or less constant in the range of 50° to 100°C. In this latter range, the relaxation frequency of the composite stabilizes surrounding 50 Hz.[39] This is the value of the relaxation frequency found in all our measurements (Fig. 2–**??**) whereas all the samples have been mixed and heated during 200 h at 100°C.

All the curves present a peak around the relaxation frequency 50 Hz. This peak is due to interfacial and orientation polarizations. The appearance of another peak around 35 Hz in the frequency curves (permittivity, loss factor and loss index) of XLPE is probably due to the effect of the chelating agent integrated into the XLPE molecule such carried out in the literature.[34,43] The cross-linking has been effectively characterized by XRD (see Fig. 8). This one contributes therefore to increase the crystallinity percentage of the composite such as carried out in Ref. 34. For a given aging temperature, the loss factor is characterized by the presence of peaks due to relaxation movements (rotation, vibration, translation) chain segments of XLPE. Thermal aging has so a significant influence on the value of the loss index. This can be explained by the relative decreasing in the viscosity of the polymer and increasing of the molecular mobility induced by relaxation movement chain segments of XLPE such as indicated in other work.[44] The relaxation peak shifts towards higher frequency, (Fig. 4) such found in the literature.[21] Noting [Fig. 4(c)] that, the concentration of $BaTiO_3$ particles influences a systematic variation of the loss maximum. The intensity of the peak diminishes with the increase of $BaTiO_3$ content and at the same time slightly shifts towards lower frequencies at the higher concentrations. The obtained results are so in agreement with that one of Refs. 15 and 39. Relaxation phenomena were found in all the examined systems. It can be attributed mainly to interfacial polarization or MWS effect, of the macromolecular chains such reported in the literature[5] in addition of relaxation due to $BaTiO_3$ as inter-granular phase in the composite

5. Conclusions

The results obtained in these investigations concerning the XLPE composite are summarized as follows.

$BaTiO_3$ loaded XPLE has been studied. The composites aged at 100°C during 200 h and immersed during 72 h in water have been analyzed. The dielectric parameters were measured. ε_r of pure XPLE was evaluated between 2.27 and 6.5, respectively at 300 Hz and 50 Hz. However, ε_r of composite has been evaluated in the range 2.2 to 7.25 if temperature and humidity effects are taken account. ε_r increases with the filler increasing and decreases on the order of 3% for the heat-treated composites. Finally, the permittivity of the composite has been evaluated in the range of values required for that one of organic polymers. The permittivity of XLPE composite was weakly sensitive to that one of $BaTiO_3$. $BaTiO_3$ as nano-filler increases so ε_r and significantly reduces $tg\delta$ and index loss in the samples strongly doped (15%wt and 20%wt). However, water diffusion in the composite decreases with increasing of $BaTiO_3$ content from 5%wt to 10%wt. Enhancing of water absorption otherwise was greater for the samples four and five whereas these one contained fissures and pores; consequently more voids more water storage is; therefore the loss index was greater than that of the unloaded sample. The storage of water in the bulk of the samples is due to fissure in the samples containing more

than 10%wt $BaTiO_3$. The losses were three times lower in 20% $BaTiO_3$ loaded sample. Otherwise the absorbed humidity and the thermal aging contribute to increasing ε_r and $tg\delta$, therefore the dielectric losses. The relaxation frequencies have been evaluated. The intensity of the relaxation peak diminishes with increasing of $BaTiO_3$ content and at the same time slightly shifts to lower frequencies at the higher concentrations. The relaxation has been found stable and located at 35 and 50 Hz frequencies respectively closer to the network frequency (50/60 Hz) resulting of temperature range treatment (100°C). The dielectric properties of composites (ε_r, $tg\delta$ and loss index) after a cycle heating/cooling are remained stable. Thermal aging effect has been occurred rather on the unloaded sample before doping and the sample four containing fissures. The incorporation of $BaTiO_3$ does not modify the crystallinity and morphology of the XLPE. $BaTiO_3$ as nano-filler reduces so the space charges accumulation (due to aggregates or small voids or pores) and decreases the breakdown probability of the composite if the doping is smaller than 15%wt. The results found closer to that of Ref. 10 show that the combination of polymer advantages and special characteristics of $BaTiO_3$ leads to improvement of XLPE dielectric properties. Finally, in order to increase the breakdown field of the composite, it is necessary and indispensable in first to master the elaboration process of the composite allowing to reach the lower cumulative probability of failure for a given electric field. Relaxation phenomena and many range of temperature will be studied in the next paper.

References

1. K. Chonung, J. Zhijian and J. Pingkai, *Polym. Test.* **25**, 553 (2006).
2. J. Gonzalez-Benito *et al.*, *Polym. Test.* **32**, 1342 (2013).
3. M. S. Khalil *et al.*, *IEEE Trans.* **3**, 743 (1996).
4. International Standard Norme, Common test methods for insulating and sheathing materials of electric cables, IEC 60811-3-2, 2nd edn, (2005), p. 10.
5. W. Kasprzak *et al.*, *Mater. Sci.* (*Poland*) **27**(4/2), 1219 (2009).
6. P. Barber, S. Balasubramanian and Y. Anguchamy, *Materials* **2**, 1697 (2009).
7. Z. Wang *et al.*, *IEEE Trans. Dielectr. Electr. Isol.* **19**, 960 (2012).
8. E. H. Immergut, W. McDowell and J. Brandrup, *Polymer Handbook* **2**, 2881 (2003).
9. Y. Ke *et al.*, *J. Appl. Phys.* **113**, 1 (2013).
10. J. F. Lomax *et al.*, *Smart. Mater. Struct.* **21**, 0850179 (2012).
11. J. Adam *et al.*, *Nanotechnology* **25**(6), 065704 (2014).
12. D. Armentrout, M. Kumosa and L. Kumosa, *IEEE Trans. Dielectr. Electr. Insul.* **11**, 506 (2004).
13. B. Minghui, Y. Xiaogen and H. Junjia, *Physica B* **14**, 2885 (2011).
14. T. Seguchi *et al.*, *Radiat. Phys. Chem.* **80**, 268 (2011).
15. J. Paul, H. Eddy Walther and J. Roots, *Polym. Degrad. Stab.* **97**, 2403 (2012).
16. S. T. Sushree and A. M. Raichur, *J. Disper. Sci. Tech.* **29**, 230 (2008).
17. H. S. Lee *et al.*, *J. Am. Ceram. Soc.* **90**, 2995 (2007).
18. J. C. Fothergill, *IEEE Trans. Electr. Insul.* 18, 1544 (2011).
19. S. F. Mendes *et al.*, *J. Mater. Sci.* **47**(3), 1378 (2012).
20. Patsidis A and G. C. Psarras, *Express Polym. Lett.* **2**, 718 (2008).
21. M. C. Félix and M. Maitrot, *J, Rev. Phys. Appl.* **13**, 5 (1978).

22. A. Nevenka and R. Stojan, *Bull. Chem. Technol. Maced.* **21**, 17 (2002).
23. A. K. Jonscher, *J. Appl. Phys.* **32**, 57 (1999).
24. K. P. Dillip, R. N. P. Choudhary and B. K. Samantaray, *Int. J. Electrochem. Sci.* **3**, 597 (2008).
25. T. Om Prakash and K. S. Anjani, *Adv. Studies Theor. Phys.* **2**, 637 (2008).
26. M. De Frutos and J. Retes, *Eur. Polym. J.* **41**, 2824 (2005).
27. H. S. B. Elayyan and S. N. Al-Refaie, *Proc. Scie. Meas. Technol.* **150**, 141 (2003).
28. L. Jianying and O. ZhaoBenhong, *IEEE Trans. Dielectr. Electr. Insul.* **18**, 1562 (2011).
29. M. C. Blanco Lo Pez, B. Rand and F. L. Riley, *J. Eur. Ceram. Soc.* **20**, 107 (2000).
30. A. Choudhury, *Mater. Chem. Phys.* **121**, 280 (2010).
31. K. N. Edward *et al.*, *J. Phys. Chem. C* **112**, 9659 (2008).
32. W. Camacho and S. Karlsson, *J. Appl. Polym. Sci.* **85**, 321 (2002),
33. C. R. Anil Kumar *et al.*, *Polym. Test.* **22**, 313 (2003).
34. S. Nilsson, T. Hjertberg and A. Smedberg, *Euro. Polym. J.* **46**, 1759 (2010).
35. C. Zhang *et al.*, *Mater. Lett.* **59**, 3648 (2005).
36. K. Jun-Gyu *et al.*, *Ceram. Int.* **30**, 2223 (2004).
37. A. Mohammed *et al.*, *J. Electron. Package* **134**, 8 (2012).
38. S. Andrea, A. Toselli and F. Pilati, *Polym. Degrad. Stab.* **96**, 2080 (2011).
39. M. A. Alam and M. H. Azarian, *Microelectron. Reliab.* **51**, 946 (2011).
40. J. Òrrit *et al.*, *J. Electrostat.* **69**, 119 (2011).
41. X. Luo, L. Chen and X. Chen, *J. Mater. Sci. Technol.* **20**, 441 (2004).
42. S. P. Mahapatra, D. K. Tripathy and Y. Lee, *Poly. Bull.* **68**, 1965 (2012).
43. M. C. Lanc *et al.*, *J. Non-Cryst. Solids* **353**, 4462 (2007).
44. A. Boubakeur and Y. Mecheri, *Ann. Chim. Sci. Mat.* **25**, 457 (2000).